Springer

KSME

Journal of Mechanical Science and Technology 27 (7) (2013) 1923~1931
www.springerlink.com/content/1738-494x
DOI 10.1007/s12206-013-0505-0

Numerical calculation of irregular tire wear caused by tread self-excited vibration and sensitivity analysis †

Hai-bo Huang[1,*], Yi-Jui Chiu[1] and Xiao-xiong Jin[2]

[1]*Faculty of Mechanical Engineering and Mechanics, Ningbo University, Ningbo, 315211, China*
[2]*College of Automotive Engineering, Tongji University, Shanghai, 201804, China*

(Manuscript Received September 21, 2012; Revised January 14, 2013; Accepted January 30, 2013)

Abstract

Tire wear negatively affects vehicle safety and riding comfort. Abnormal wear is more dangerous and wears tires out more quickly. In this paper, numerical and sensitivity analyses of polygonal wear caused by unstable vibration are presented. The model used for this study was based on the works of Sueoka. Tread self-excited vibration was analyzed in a quantitative sense, which was qualitatively different from the work of Sueoka. Wear was plotted on tire circumference visually. The mechanism governing polygonal tire wear was investigated as that both the polygonal wear and the standing wave are caused by two types of tread vibrations that only differ in the extent of the tread vibration. Sensitivity analysis shows that decreases in tread mass and stiffness and increases in tread damping lead to noticeable reductions in tire wear. This information could help tire manufacturers produce tires that exhibit less wear caused by tread vibration.

Keywords: Tire; Polygonal wear; Numerical analysis; Sensitivity analysis; Unstable vibration

1. Introduction

Tire wear is a complex phenomenon that is affected by tire materials, structures, vehicle dynamics, and road conditions [1-6]. There are many approaches to a tire wear study, such as finite element method (FEM) and analytical method. With the advancement of computer technology and finite element techniques, FEM has been widely used in tire wear prediction [7-12]. The pattern shape, cross-section shape and tire structure parameters can be discussed or optimized to predict and reduce tire wear. Theoretical models have been developed for tire wear and vibration. The papers [13-20] treated theoretical models of different types of tire wear, which focused on the physical processes of wear, the vibration modes of the tire and interaction between the tire and road, and so on. Theoretical models are helpful in understanding numerical results with physical mechanisms which are responsible for the generation of tire wear and their behavior at different values of tire parameters.

Abnormal wear, which is more critical for its safety implications, includes two types: uneven wear and irregular wear. Uneven wear describes non-uniform distribution of wear across tread pattern and irregular wear mainly characterizes circumferential wear variation.

In mechanical engineering, some rotating contact systems are used, such as rotor system, pulley-belt system and tire-ground system. Sometimes the peripheral surface of a roll is disturbed by random excitation. It will excite the surface of the rotating object to vibrate unstably. When unstable vibration appears by continuous excitations, it will make the object surface to wear irregularly and fail earlier. The contact of tire and ground is a classic rotating surface contact system, and elasticity of tire rubber is bigger than that of steel or iron. There is a strong possibility of occurrence of this phenomenon. One kind of tire irregular wear is polygonal wear in circumferential direction, and the number of polygonal edges is about 10-20. The polygonal wear often occurs on idle wheels irrespective of tread pattern of tire, and the wear pattern seems to be slightly oblique to the axial direction of tire.

Suoeka et al. [17] explained that this kind of polygonal tire wear was induced by forced displacement and tread self-vibration. They analyzed the mechanism of polygonal tire wear of truck, bus and car. The characteristic equations of his model for irregular wear were dealt with by Laplace transformation, and it was verified that the tire polygonal wear would appear when there were unstable characteristic roots with positive real parts. Sawant [18] added the mass of the driver into Suoeka's tire wear model and used the same method to study the polygonal tire wear. Ren [19] investigated tire irregular wear of the driven wheel, which was caused by periodic vibration of power-transmission system. His works

*Corresponding author. Tel.: +86 574 87600534, Fax.: +86 574 87608358
E-mail address: huanghaibo@nbu.edu.cn
† Recommended by Associate Editor Cheolung Cheong

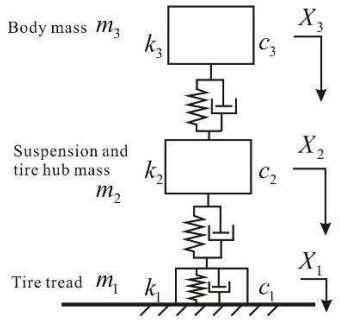

Fig. 1. Schematic of the one quarter vehicle model.

showed that unstable vibration would happen when the driven wheel slip ratio was over one specific value, and torsion vibration of the driven wheel would occur in the power transmission system. Then the irregular wear of the driven tire might appear. Zhou [20] explored polygonal tire wear caused by tread lateral self-excited vibration. He built a tread lateral slip vibration model and found that the vibration was one stable limit cycle vibration after Hopf bifurcation. All these works presented the mechanism of tire polygonal wear occurrence from the view of Lyapunov dynamic stability theory and self-excited vibration theory using Laplace transformation method. They gave the stability condition of the system in a qualitative sense. Nevertheless, they did not describe the phenomenon quantitatively. And, how tire parameters affect the polygonal wear has not yet been dealt with.

In this paper, quantitative analysis and sensitivity analysis of polygonal wear caused by tire tread unstable vibration were carried out. The equations of instantaneous wear caused by unstable vibration were deduced in detail for wear calculation in time domain. The method for circumferential wear calculation was introduced. The theoretical model was solved in time history in a quantitative sense and the tire wear was shown in tire periphery visually. Additionally, sensitivity analysis was also explored to investigate the influence of tire physical parameters on this kind of irregular tire wear.

2. Theoretical analysis

2.1 Assumption

The system is built as a vertical vibration system with lumped mass. It is a 3-DOF, one quarter vehicle system model that vibrates only in the vertical direction, as shown in Fig. 1. This system is different from the classic vibration system in which the stiffness of the tire tread and the side wall are regarded as independent elements in the vibration. The stiffness variables include three elements: the tread, the side wall and the suspension spring. The definition of m_1, k_1, c_1, m_2, k_2, c_2, m_3, k_3 and c_3 can be easily understood in Fig. 1. There are also some important assumptions and simplifications listed below that will be helpful for readers to understand the background and modeling process.

(1) The polygonal tire wear often happens in high way driving because it is possible that the vehicle drives straight and at constant velocity for a long time. This paper doesn't discuss the wear caused by transient state driving, such as braking and cornering.

(2) Wear includes two parts. The first is the amount of wear before one period, which we represent as $H(t-T)$, where T is the time period during which the tire is rotating. The other part $I(t)$, is the amount of instantaneous wear at time t. The total amount of wear loss $H(T)$ at time t is

$$H(t)=H(t-T)+I(t). \tag{1}$$

A self-excitation process is generated via forced displacement $I(t)$, and energy produced in this process prevents the tread vibration from weakening. Moreover, due to idle tire and assumption (1), the tire wear is mainly caused by the lateral force $F(t)$, which is the function of vertical load:

$$F(t)=(a_\gamma\times\gamma-a_\alpha\times\alpha)P(t) \tag{2}$$

where a_γ, a_α are the linear constants for camber γ and toe α, respectively, and $P(t)$ is the instantaneous vertical force between the tire and road. The contact vertical force is

$$P(t)=P_0+c_1(\dot{X}_1(t)-\dot{H}(t-T))+k_1(X_1(t)-H(t-T)) \tag{3}$$

where P_0 is the sum of the sprung and un-sprung gravitational forces. Contact force $P(t)$ is always positive.

(3) The amount of instantaneous wear is computed by using the following equation:

$$I(t)=\upsilon\times F(t)=\upsilon\beta^n[P(t)]^n \tag{4}$$

where $\beta=\left|a_\gamma\times\gamma-a_\alpha\times\alpha\right|$. υ is the reciprocal of wear resistance of the tire. n is the power of law. υ and n are both determined by the roughness of the road and tire materials. Corresponding to the wear theory of Schallamach [17], $n=2$ is preferred in the paper. The wear coefficient υ is set to 2.4×10^{-13} (m/N) for vibration-induced wear, which is bigger than the value of even wear for one order of magnitude. It is helpful to show the phenomenon more clearly.

2.2 The theoretical model

When tire wear occurs, wear loss will compress tread spring. Based on the assumption in section 2.1, the system steady-state vibration equations are

$$\begin{cases} m_1\ddot{X}_1(t)+c_2[\dot{X}_1(t)-\dot{X}_2(t)]+k_2[X_1(t)-X_2(t)]+ \\ c_1[\dot{X}_1(t)-\dot{H}(t-T)]+k_1[X_1(t)-H(t-T)]=0 \\ m_2\ddot{X}_2(t)+c_2[\dot{X}_2(t)-\dot{X}_1(t)]+k_2[X_2(t)-X_1(t)]+ \\ c_3[\dot{X}_2(t)-\dot{X}_3(t)]+k_3[X_2(t)-X_3(t)]=0 \\ m_3\ddot{X}_3(t)+c_3[\dot{X}_3(t)-\dot{X}_2(t)]+k_3[X_3(t)-X_2(t)]=0 \\ H(t)=H(t-T)+\upsilon\beta^n\{P_0+c_1[\dot{X}_1(t)-\dot{H}(t-T)]+ \\ k_1[X_1(t)-H(t-T)]\}^n \end{cases} \tag{5}$$

where X_i, $\dot{X}_i$ and $\ddot{X}_i$ are the stable vibration displacement, velocity and acceleration, $i = 1,2,3$.

When $t < T$, there is no wear on the tire before the tire finishes the first rotation, so

$$H(t-T) = 0,\ \dot{H}(t-T) = 0, \text{ when } t < T \tag{6}$$

The model equation in steady state is

$$\begin{cases} M\ddot{X}(t) + C\dot{X}(t) + KX(t) = V(t) \\ H(t) = H(t-T) + \upsilon\beta^n\{P_0 + c_1[\dot{X}_1(t) - \dot{H}(t-T)] + \\ k_1[X_1(t) - H(t-T)]\}^n \\ H(t-T) = 0,\ \ \dot{H}(t-T) = 0, t < T. \end{cases} \tag{7}$$

The element matrices are listed in Appendix A.1, (A1) - (A5).

The steady-state solutions $X_{10}(t)$, $X_{20}(t)$, $X_{30}(t)$ and $H_0(t)$ are presented by using the variables with subscript 0 and can be obtained by putting $P(t)$ equal to P_0 in Eq. (4). Then, the steady-state wear can be computed as

$$\begin{cases} H_0(t) = \upsilon\beta^n P_0^n (t+T)/T \\ X_{10}(t) = H_0(t-T) = \upsilon\beta^n P_0^n t/T. \end{cases} \tag{8}$$

When the tread is disturbed by external excitation, it begins to vibrate and wear amount will be different in the steady state. Here, the variables $x_1(t)$, $x_2(t)$, $x_3(t)$ and $h(t)$, are expressed by using the small letter corresponding to the variables of capital letter as

$$x_i(t) = X_{iU}(t) - X_{i0}(t) \quad h(t) = H_U(t) - H_0(t) \quad i = 1, 2, 3 \tag{9}$$

where $X_{iU}(t)$ and $H_U(t)$ are the solution of the unstable vibration system, presented using the variables with subscript U. Substituting Eq. (9) into Eqs. (7) and (8) yields the following equation

$$\begin{cases} M\ddot{x}(t) + C\dot{x}(t) + Kx(t) = Q(t) \\ h(t) = h(t-T) + i(t). \end{cases} \tag{10}$$

The element matrices are listed in Appendix A.1, (A6) - (A7). The tire tread sometimes vibrates opposite to the road and there is no extra wear on the tire in such cases, so there are some limitations on instantaneous wear amount $i(t)$. Taking Eqs. (3), (4) and (8) into account, we obtain

$$i(t) = \begin{cases} i_e(t) & i_e(t) \geq 0 \\ 0 & i_e(t) < 0 \end{cases} \tag{11}$$

$$i_e(t) = \upsilon\beta^n P_0^{n-1} n\{c_1[(\dot{x}_1(t) - \dot{h}(t-T)] + k_1[x_1(t) - h(t-T)]\}. \tag{12}$$

The detailed derivation process for $i_e(t)$ is listed in Appendix A.2. Eq. (10) is the system disturbed equation. Using this equation, the polygonal wear caused by tread vibration can be calculated. The equation includes time delay elements, which is influenced by the rotation frequency and the tire's physical parameters.

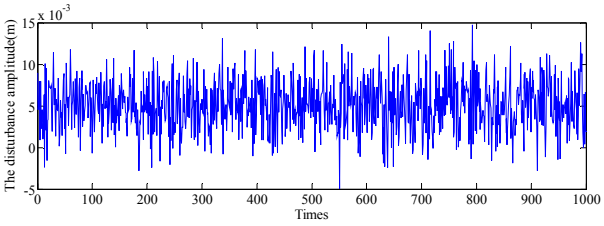

Fig. 2. The random disturbed amplitudes.

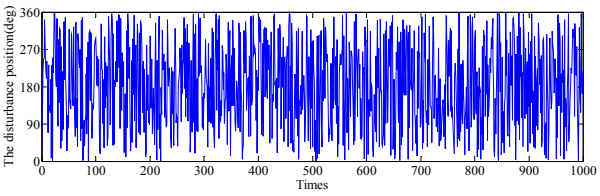

Fig. 3. The random disturbed positions.

3. Numerical results and discussion

3.1 The amplitude and position of disturbed excitation

Disturbed excitation is affected by environment, road roughness and tire structure. It is unrepeatable and uncertain [21]. Neither instantaneous disturbed amplitude nor excited position of tire can be predicted in a deterministic sense. Two groups of random signal are employed to generate the excited amplitudes and positions. The disturbed amplitudes generally have values close to a mean, although a small number of other amplitudes have values significantly above or below it. Accordingly, the amplitudes of the excitation for the model are regarded as a group of Gaussian distribution signals $N(0.005, 0.3)$ with a mean of 0.005, a variance of 0.3 at interval $[0, 0.015]$ and a significance level of 0.9, as shown in Fig. 2.

The tire's excitation position in tire circumferential direction is also uncertain. Since the positions tend to be equally distributed around the tire circumference, the excitation positions are regarded as a group of uniform distribution signals at interval $[0^\circ, 360^\circ]$. The random positions of 1,000 times of excitations around tire circumference are shown in Fig. 3.

Tire excitation is affected by many factors, and it is difficult to determine the frequency of the excitation. For simplification, disturbed excitation occurs once per tire rotating circle, but the excitation amplitude and position are random. When the tread is disturbed, the excitation is so small that tread vibration just attenuates in one rotation cycle, which will be explained in section 3.3.

When the amplitude is applied as a tread displacement, the tread begins to vibrate and the disturbance happens. The wear

Table 1. Simulation parameters.

symbol	Description	Value
m_1	Tread mass	2.3 Kg
m_2	Suspension mass	17.5 Kg
m_3	Body mass	300 Kg
c_1	Tread damping	98 N·s/m
c_2	Sidewall damping	147 N·s/m
c_3	Suspension damping	1181 N·s/m
k_1	Tread stiffness	941,000 N/m
k_2	Sidewall stiffness	299,000 N/m
k_3	Suspension stiffness	14,700 N/m
r	Tire radius	0.32 m
n	The power of law	2
υ	The reciprocal of wear resistance	4.76×10^{-14}m/N
γ	Camber	1.5°
a_γ	The linear constant for camber	0.014 1/deg
α	Toe	0.3°
α_α	The linear constant for toe	0.22 1/deg

caused by tread vibration appears in the tire circumferential direction. Based on Ref. [17] and the tests conducted, the parameters are listed in Table 1.

3.2 The method for circumferential wear calculation

The model presented is used to calculate the contact wear between tire tread and road. It indicates wear at a point and cannot be used to determine the amount of wear distributed around the tire circumference. However, when the time step Δt is constant, the wear point positions will be distributed evenly along the tire circumference. The number of wear points D on the tire circumference will be

$$D = \frac{T}{\Delta t} \tag{13}$$

where T is the rotation period. Tire rotation is a continuous process, and the wear values should be added for each rotation at each position. To solve the problem, the positions on tire periphery are numbered, and the number for each position is unique. Due to constant velocity and time step, the wear positions are distributed evenly on the tire circumference. When the disturbed vibration starts at position i, i is the serial number; the wear caused by the vibration will occur at the following points, such as at position $i+1$, $i+2$, $i+3\ldots$ until where vibration attenuates and disappears. The total wear at i position after the vibration will be the sum of $W'(i)$ caused by former rotations and $w(i)$ caused by this time. Likewise, the total wear at $i+1$ position will be the sum of $W'(i+1)$ caused by former rotations and $w(i+1)$ caused by this time. Therefore, the wear for additional rotations can be obtained and irregular wear can be determined.

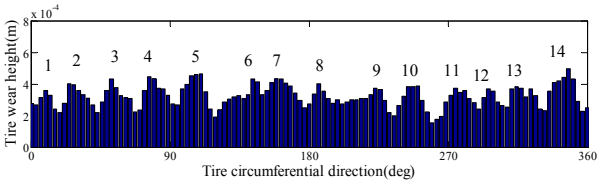

(a) The lateral view of tire wear amount

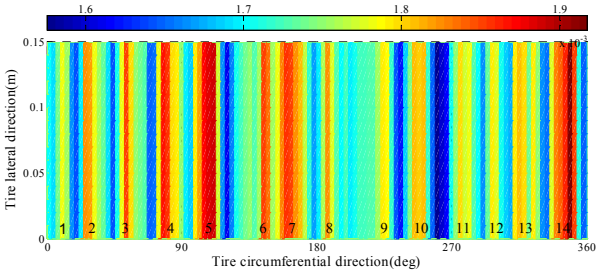

(b) The top view of the tire wear amount

Fig. 4. Wear amount from different views when the vehicle is traveling at 60 km/h for 30,000 km.

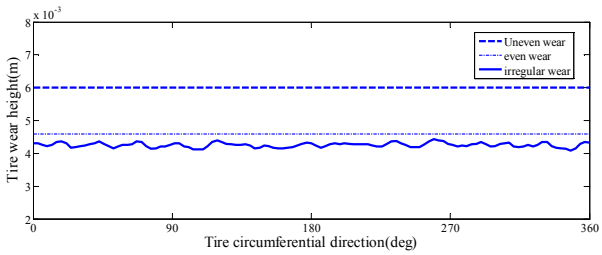

Fig. 5. The wear amount of even wear and uneven wear when vehicle is traveling at 60 km/h for 30,000 km.

3.3 The simulation results

We used the linear acceleration method to solve the formulation. We assumed that the tire runs 30,000 km at 60 km/h. The tire rotation period T is 0.12 s, and the angular velocity is 52.6 rad/s. The total amount of polygonal wear is illustrated in Fig. 4 in the lateral view and circumferential direction.

As shown in Fig. 4, several peaks of wear appear and the wear is polygonal on the tire circumference. The values of the peaks are not significantly different, and the peak positions are distributed on the tire circumference roughly and evenly. The number of peaks is approximately 14.

The amounts of even wear, irregular wear and unworn tire are given in Fig. 5, which shows that the tire wear is mainly the even wear. The amount of the even wear is approximately 1.5 mm and the amount of the polygonal wear is approximately 0.5 mm. The wear amount is sufficient to show the local wear on the tire periphery.

Under normal conditions, the unworn height of the tire tread is 6 mm, and the tire is junked once the remaining tread height is 1.5 mm. From Eq. (4), the life of a tire is approximately 90,000 km without tread vibration in theory. If wear caused by tread vibration happens, the life of the tire will be less than 60,000 km.

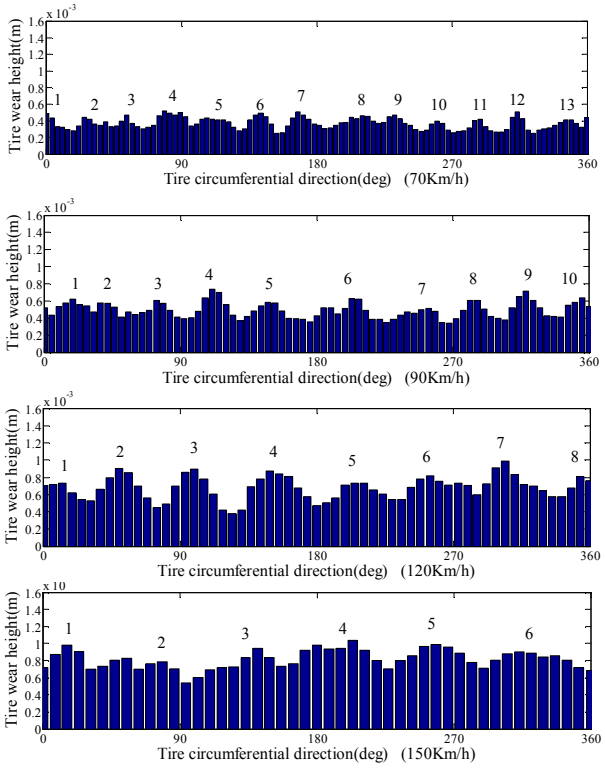

Fig. 6. The wear amounts at the usual velocities of 70, 90, 120 and 150 km/h for 30,000 km.

3.4 Simulations under different velocities

From the results above, there are approximately 14 wear peaks in the tire circumference when the vehicle is driven at 60 km/h. Simulations must be conducted at different velocities to determine whether irregular wear exhibits regularity and periodicity. The wear at usual velocities of 70 km/h, 90 km/h, 120 km/h and 150 km/h has been calculated as shown in Fig. 6.

Fig. 6 shows that at different velocities, there are wear peaks in local tire regions that cause the tire circumference to be polygonal. The numbers identify the sequence of wear peaks. The number of peaks is related to the vehicle velocity, which is greater with lower velocity. Under the same conditions, the wear is much more severe when the vehicle is driven at a higher speed.

3.5 The mechanism of the uneven wear caused by tread vibration

In Ref. [17], tire tread vibration is understood as self-excited vibration created by random excitations. The disturbed frequency is the tire's vertical natural frequency f. The number of the polygonal edge of wear N is expressed as

$$N \approx 2\pi f / \omega \tag{14}$$

where ω is the tire's rolling speed, and

Table 2. Velocity, frequency and peak number.

Vehicle velocity (km/h)	60	70	90	120	150
Tire angular velocity ω (rad/s)	52.6	61.3	78.9	105.2	131.4
Tire rotation frequency (Hz)	8.4	9.7	12.5	16.7	20.92
The theoretical results for the peak number	13.97	11.97	9.3	6.98	5.58
The simulation results for the peak number	14~16	12~13	9~10	7~8	5~6

$$f \approx \frac{1}{2\pi}\sqrt{\frac{k_1 + k_2}{m_1}} \tag{15}$$

$$\omega = 2\pi / T\ . \tag{16}$$

In Eq. (14), when the tread's natural frequency is higher and the vehicle's velocity is lower, the polygonal edge number will be greater. The theoretical results determining the number of peaks, which are listed in Table 2, are consistent with the results in Fig. 6.

The tire surface exhibits different types of wear due to various velocities. When the vehicle velocity is always within a certain range, the number of polygonal edges will be predominantly observable type in accordance with that velocity.

As a tire always runs at a constant and high speed and is disturbed by road roughness, polygonal wear may occur. Under these conditions, the disturbed vibration weakens and disappears in one rotation. When tire tread vibration continues to the next rotation, a phenomenon similar to the "standing wave" may occur. Under these conditions, the tire velocity is extremely high.

4. The sensitivity analysis

The tire's structural parameters will influence tire wear greatly. By modifying these structural parameters one at a time and considering the tread characteristics, we can conduct simulations to compare the effects of different parameters on the polygonal wear. In this case, it is assumed that a tire runs at 70 km/h for 30,000 km. The parameters are changed one at a time by intervals of $\pm 25\%$ to compute the tire's average wear $W_{average}$. In each simulation, the group of excitation amplitudes is the same, but the excited positions are regenerated according to the uniform distribution each time. The average wear considers the wear points around the tire and is defined as

$$W_{average} = \frac{\sum_{m=1}^{D} W_p(m)}{D} \tag{17}$$

where D is the number of wear points around the tire based on Eq. (13). $W_p(m)$ is the amount of wear at one point caused by unstable vibration.

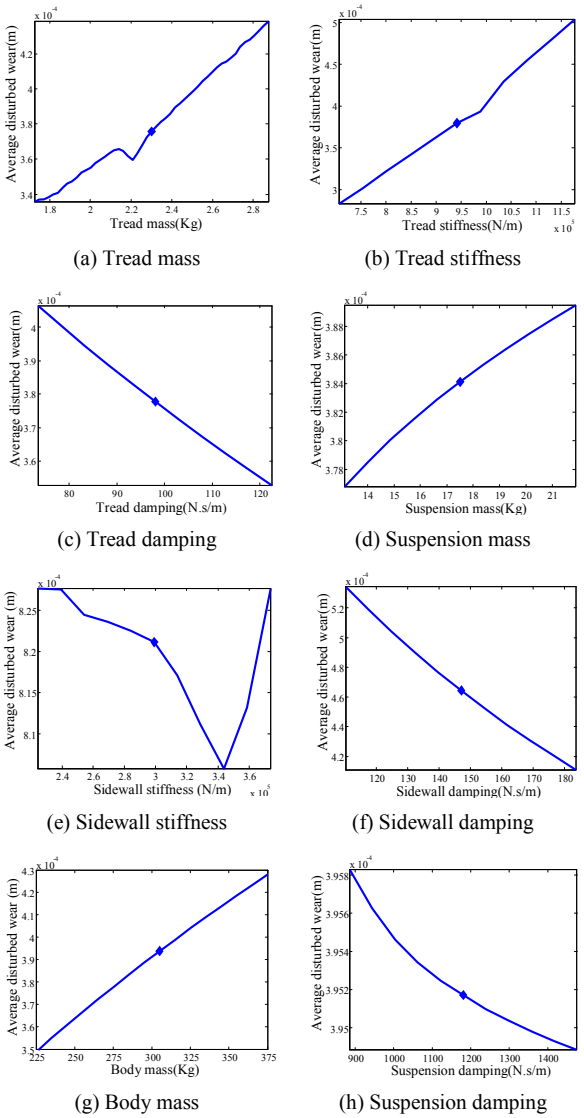

(a) Tread mass (b) Tread stiffness

(c) Tread damping (d) Suspension mass

(e) Sidewall stiffness (f) Sidewall damping

(g) Body mass (h) Suspension damping

Fig. 7. Average wear diagram different variables values.

The simulation results of different variables are listed in Fig. 7. The solid lines indicate the calculation results, and the diamond symbol indicates the initial value. The randomness of the results is eliminated by using several computations. Significant guidance quality of most plots is represented by either ascending or descending results without inflection points. From Fig. 7, a particular increase in one parameter does not lead to the same decrease or increase in the wear amount, thus indicating the presence of nonlinear effects.

Fig. 7(a) shows the relationship between average wear amount and the tread mass. It can be seen that an increase in tread mass will accelerate a tire's irregular wear generally. Similarly, average wear amount increases with the tread stiffness, as shown in Fig. 7(b). There is a small inflection point in Figs. 7(a) and (b) each, but both the inflection points are not significant and the influence trends on the results do not change.

Table 3. Effects of changes to structural parameters on tire wear.

symbol	-25%	+25%	symbol	-25%	+25%
m_1	-10.51%	17.40%	c_1	6.08%	-7.93%
m_2	-1.56%	1.71%	c_2	11.95%	-13.78%
m_3	-10.21%	10.19%	c_3	0.14%	-0.09%
k_1	-20.53%	40.79%	k_2	/	/
k_3	0.006%	-0.008%			

The average wear amount is shown as a function of tread damping in Fig. 7(c). From this data, the wear amount decreases almost linearly with the tread damping increasing. As expected, Fig. 7(d) shows that the wear amount increases as the suspension mass increases.

Fig. 7(e) indicates the relationship between the wear amount and the sidewall stiffness. It is interesting that there is an inflection point for the results. The influence of sidewall stiffness on average disturbed wear is clearly different on the left and right of the inflection point. The wear increases on the right of the inflection point but exhibits a relatively gradual decline on the left. When the sidewall stiffness is set to 3.50×10^5 N/m (with an initial value of 2.99×10^5 N/m), the average disturbed wear is at the minimum value of 8.02×10^{-4} m. Together with the small inflection points in Figs. 7(a) and (b), what caused the inflection points is not clear, but it is conjectured that it is related to the vibration frequency of the tire tread.

Fig. 7(f) shows that the sidewall damping affects the average wear amount. With increasing sidewall damping, the average wear amount will decrease. The results of the average wear loss versus body mass are illustrated in Fig. 7(g) which shows that the average wear loss increases with greater body mass. Fig. 7(h) shows that increased suspension damping will insignificantly decrease the wear amount.

Table 3 shows the change in wear amount (as a percentage) associated with different parameters that is obtained by changing those parameters by $\pm25\%$. The values are the average values obtained from three times of computations to eliminate randomness. Increasing the damping of the tread, sidewall and suspension leads to a decrease of -7.93%, -13.78%, and -0.09% in the amount of wear, respectively. The body mass, tread mass, tread stiffness, sidewall damping and tread damping have the greatest effect on the amount of wear, in that order. With increasing of the first three, the average wear amount will decrease by 10.19%, 17.40% and 40.79%, whereas the increases of the last two will decrease wear amount at a rate of -13.78% and -7.93%. Stiffness and suspension damping of the body have less effect on the amount of wear.

Increase in tread mass and stiffness creates a greater vertical excitation force, thus leading to greater irregular wear. Increased tread damping leads to less time of disturbed vibration, thus leading to less wear amount. However, these improvements are achievable only when we keep the other parameters of the tire constant. Nevertheless, this paper provides quantita-

tive information about which tire parameter best reduces the tire wear.

5. Conclusions

We have presented a theoretical wear model induced by forced unstable vibration in tires. The proposed tire model makes it possible to predict the polygonal tire wear both qualitatively and quantitatively. The mechanism of polygonal tire tread wear is also reinterpreted here compared to Ref. [17]. It is similar to the "standing wave" phenomenon, but the vibration intensity is weaker than that in the latter case. It is attenuated within one rotation, while the tread is continuously oscillating more than one cycle in "standing wave." These two phenomena differ from variations in the extent of tread vibration.

The conditions that cause polygonal tire wear are also discussed. If the tread is disturbed by external excitation and vibrates continuously, polygonal tire wear probably occurs. Because of the high degree of stiffness and damping, tire tread usually does not continue to vibrate. Therefore, polygonal tire wear does not occur with most tires. However, the phenomenon still occasionally happens. It may be caused by regular gaps between sections of pavement or other regular excitations.

Moreover, a numerical procedure for determining the effect of vehicle parameters on tire wear is studied here. A series of model simulations are generated by varying each single parameter of the tire model by ±25%. The sensitivity analysis shows that tread properties have the greatest influence on tire wear. A decrease in tread mass and stiffness and an increase in tread damping will lead to a sizeable reduction in tire wear (with reductions of approximately -10.51%, -20.53% and -7.93%, respectively).

It is interesting that the results have inflection points in Figs. 7(a), (b) and (e). The parameters represented in these figures, tread mass, tread stiffness and side stiffness, are strongly correlated with tread vibration and can cause significant changes in tire wear, especially in the number of polygonal edges of wear. Future research should determine the mechanisms governing the inflection points.

Acknowledgments

We gratefully acknowledge the National Natural Science Foundation of China (Grant No. 51205213) and Talent Fund of Ningbo University, China for both financial supports. The work was also sponsored by the K.C.Wong Magna Fund in Ningbo University.

References

[1] A. G. Veith, Tire tread wear-a comprehensive evaluation of the factors: generic type, aspect ratio, tread pattern, and tread composition, *Tire Science and Technology*, 14 (4) (1986) 219-234.

[2] K. A. Grosch, Abrasion of rubber and its relation to tire wear, *Rubber Chemistry and Technology*, 65 (1) (1992) 78-106.

[3] M. H. Waiters, Uneven wear of vehicle tires, *Tire Science and Technology*, 21 (4) (1993) 202-219.

[4] S. J. Kim and A. R. Savkoor, The contact problem of in-plane rolling of tires on a flat road, *Vehicle System Dynamics*, 27 (Sup001) (1997) 189-206.

[5] M. G. Gilbert, Effects of tire shoulder wear on vehicle roll-over limit testing, *SAE*, 2003-01-2865 (2003) 401-406.

[6] J. P. Pauwelussen, The local contact between tyre and road under steady state combined slip conditions, *Vehicle System Dynamics*, 41 (1) (2004) 1-26.

[7] K. S. Park, C. W. Oh, T. W. Kim, H. Y. Jeong and Y. H. Kim, An improved friction model and its implications for the slip, the frictional energy, and the cornering force and moment of tires, *Journal of Mechanical Science and Technology*, 20 (3) (2006) 1399-1409.

[8] J. R. Cho, S.W. Shin and W. S. Yoo, Crown shape optimization for enhancing tire wear performance by ANN, *Computers and Structures*, 83 (12) (2005) 920-933.

[9] J. C. Cho and B. C. Jung, Prediction of tread pattern wear by an explicit finite element model, *Tire Science and Technology*, 35 (4) (2007) 276-299.

[10] F. Liu, M. P. F. Sutcliffe and W. R. Graham, Prediction of tread block forces for a free-rolling tire in contact with a smooth road, *Wear*, 269 (9) (2010) 672-683.

[11] J. R. Cho, J. H. Choi and Y. S. Kim, Abrasive wear amount estimate for 3d patterned tire utilizing frictional dynamic rolling analysis, *Tribology International*, 44 (7-8) (2011) 850-858.

[12] D. W. Lee, J. K. Kim, S. R. Kim and K. H. Lee, Shape design of a tire contour based on approximation model, *Journal of Mechanical Science and Technology*, 25 (1) (2011) 149-155.

[13] H. Lupker, F. Cheli and F. Braghin, Numerical prediction of car tire wear, *Tire Science and Technology*, 32 (3) (2004) 164-186.

[14] M. Gäfvert and J. Svendenius, A novel semi-empirical tyre model for combined slips, *Vehicle System Dynamics*, 43 (5) (2005) 351-384.

[15] M. Gipser, Ftire-the tire simulation model for all applications related to vehicle dynamics, *Vehicle System Dynamics*, 45 (Sup001) (2007) 139-151.

[16] F. Braghin, F. Cheli and S. Melzi, Tire wear model: validation and sensitivity analysis, *Meccanica*, 41 (2) (2006) 143-156.

[17] A. Sueoka and R. Takahiro, Polygonal wear of automobile tire, *JSME*, 40 (series C) (1997) 209-217.

[18] P. J. Sawant and S. G. Joshi, Theoretical analysis of unstable vibration of tyre mass-suspension system with cab of a typical road vehicle, *Journal of the Institution of Engineers (India)*, 86 (2005) 38-44.

[19] S. Y. Ren, Research on dynamic traction behaviors and related problems of towing tractors under towing load, Ph.D.

Dissertation of Shanghai Jiaotong University, Shanghai, China (2004).
[20] Z. H. Zhou, S. G. Zuo and Q. Feng, Research on polygonal wear of automotive tire based on self excitation theory, *System Simulation Technology*, 4 (1) (2008) 19-24.
[21] J. Dai, W. Gao and N. Zhang, Random displacement and acceleration responses of vehicles with uncertainty, *Journal of Mechanical Science and Technology*, 25 (5) (2011) 1221-1229.

Appendix

A.1 Matrices elements

$$X(t)=\begin{Bmatrix} X_1(t) \\ X_2(t) \\ X_3(t) \end{Bmatrix} \tag{A1}$$

$$M=\begin{bmatrix} m_1 & 0 & 0 \\ 0 & m_2 & 0 \\ 0 & 0 & m_3 \end{bmatrix} \tag{A2}$$

$$C=\begin{bmatrix} c_1+c_2 & -c_2 & 0 \\ -c_2 & c_2+c_3 & -c_3 \\ 0 & -c_3 & c_3 \end{bmatrix} \tag{A3}$$

$$K=\begin{bmatrix} k_1+k_2 & -k_2 & 0 \\ -k_2 & k_2+k_3 & -k_3 \\ 0 & -k_3 & k_3 \end{bmatrix} \tag{A4}$$

$$V(t)=\begin{bmatrix} c_1[\dot{X}_1(t)-\dot{H}(t-T)]+k_1[X_1(t)-H(t-T)] \\ 0 \\ 0 \end{bmatrix} \tag{A5}$$

$$x(t)=\begin{Bmatrix} x_1(t) \\ x_2(t) \\ x_3(t) \end{Bmatrix} \tag{A6}$$

$$Q(t)=\begin{bmatrix} c_1[\dot{x}_1(t)-\dot{h}(t-T)]+k_1[x_1(t)-h(t-T)] \\ 0 \\ 0 \end{bmatrix}. \tag{A7}$$

A.2 The detailed derivation process of $i_e(t)$

The steady-state wear solution mentioned corresponds to the one obtained by putting $P(t)=P_0$ in Eq. (3). Hence, $X_1(t)$ is equal to $H(t-T)$. Considering Eqs. (3) and (9), when the tread is disturbed, the contact vertical force induced by tread unstable vibration is

$$P(t)=P_0+c_1\Big[(\dot{x}_1(t)-\dot{h}(t-T)]+k_1[x_1(t)-h(t-T)]\,. \tag{A8}$$

Suppose that

$$G=c_1[(\dot{x}_1(t))-\dot{h}(t-T)]+k_1[x_1(t)-h(t-T)]\,. \tag{A9}$$

Then,

$$P(t)=P_0+G\,. \tag{A10}$$

At time t, the total wear is the sum of the amount of stable wear and unstable wear

$$H_U\ (t)=H_0(t)+h(t)\,. \tag{A11}$$

From Eqs. (8), (9) and (10),

$$\begin{aligned} &h(t)=H_U(t)-H_0(t)=H_U(t-T)+I(t)-\upsilon\beta^n P_0^{\,n}(t+T)/T= \\ &H_U(t-T)+\upsilon\beta^n\{P_0+G\}^n-\upsilon\beta^n P_0^{\,n}(t+T)/T= \\ &H_0(t-T)+h(t-T)+\upsilon\beta^n\{P_0+G\}^n-\upsilon\beta^n P_0^{\,n}(t+T)/T\,. \end{aligned} \tag{A12}$$

From Eq. (8),

$$H_0(t-T)=\upsilon\beta^n\{P_0\}^n(t-T+T)/T=\upsilon\beta^n\{P_0\}^n t/T\,. \tag{A13}$$

Then,

$$\begin{aligned} &h(t)=H_0(t-T)+h(t-T)+\upsilon\beta^n\{P_0+G\}^n- \\ &\upsilon\beta^n P_0^{\,n}(t+T)/T=\upsilon\beta^n\{P_0\}^n t/T+h(t-T)+\upsilon\beta^n\{P_0+G\}^n- \\ &\upsilon\beta^n P_0^{\,n}(t+T)/T=h(t-T)+\upsilon\beta^n\{P_0+G\}^n-\upsilon\beta^n P_0^{\,n}\,. \end{aligned} \tag{A14}$$

Taylor series expansion is used in item $\{P_0+G\}^n$, it gets

$$\{P_0+G\}^n=P_0^{\,n}+nP_0^{\,n-1}G+\frac{n(n-1)}{2}P_0^{\,n-2}G^2\ldots+P_0G^{n-1}+G^n \tag{A15}$$

where G is the disturbed force between the road and the tread, which is so small that its high order item $\frac{n(n-1)}{2}P_0^{\,n-2}G^2$ is very small as to be ignored in the following computations. After removing the lower order of P_0 and the higher order of G, we obtain two items:

$$\{P_0+G\}^n\approx P_0^{\,n}+nP_0^{\,n-1}G\,. \tag{A16}$$

Substituting Eq. (A16) into Eq. (A14) yields

$$h(t)=h(t-T)+i_e(t)\} \tag{A17}$$

where

$$i_e(t)=\upsilon\beta^n P_0^{\,n-1}n\{c_1\Big[(\dot{x}_1(t)-\dot{h}(t-T)]+k_1[x_1(t)-h(t-T)]\}\,. \tag{A18}$$

Hai-bo Huang is now an associate professor of Faculty of Mechanical Engineering and Mechanics at Ningbo University. He received his Master's and Ph.D. in Mechanical Engineering from Shandong University, China in 2002 and Tongji University, China in 2006, respectively. His research interests include wear in rotating systems and tire dynamics.

Yi-Jui Chiu obtained his Ph.D. in Mechanical Engineering from the National Taiwan University of Science and Technology, Taiwan in 2008. He had been working at the High-Tech Facility Design and Construction Center in National Taiwan University. Now, he is working at Ningbo University, China. His research interests include rotor dynamics and structure vibration.

Xiao-xiong Jin is a professor of the automotive college of Tongji University. He got his B.S., M.S. and Ph.D. in Mechanical Engineering from Tongji University, China in 1975, 1995 and 1998, respectively. His research interests include vehicle vibration and noise control and vehicle structure durability.